ELSEVIER

Polymer 44 (2003) 101–114

polymer

www.elsevier.com/locate/polymer

# Vitrification and dielectric relaxation during the isothermal curing of an epoxy–amine resin

S. Montserrat*, F. Roman, P. Colomer

*Departament de Màquines i Motors Tèrmics, Universitat Politècnica de Catalunya, Carrer de Colom 11, 08222 Terrassa, Spain*

Received 4 July 2002; received in revised form 26 September 2002; accepted 10 October 2002

**Abstract**

The isothermal curing of an epoxy resin based on diglycidyl ether of bisphenol A (DGEBA) with a diamine based on 4,4′-diamino-3,3′-dimethyldicyclohexylmethane (3DCM) was analysed by dielectric relaxation spectroscopy (DRS), conventional differential scanning calorimetry (DSC) and temperature modulated DSC (TMDSC). The chemical kinetics corresponds to an autocatalytic model with an apparent activation energy of 58 kJ mol$^{-1}$. The vitrification was analysed by TMDSC, between 40 and 140 °C, using the modulus of the complex heat capacity, $|C_p^*|$. A mobility factor based on the evolution of $|C_p^*|$ was used to study the reaction step controlled by diffusion. The permittivity and loss factor were measured by DRS as a function of time in the frequency range between 10 Hz and 100 kHz. The dipolar relaxation, analysed by the peak of the maximum loss factor, was correlated with the vitrification determined by TMDSC. The analysis of the logarithm of the frequency against the conversion degree allows the characterisation of the molecular dynamics of the crosslinking reaction up until the vitrification of the system.


*Keywords:* Curing reaction; Temperature modulated differential scanning calorimetry; Dielectric relaxation spectroscopy

## 1. Introduction

The crosslinking reaction of an epoxy–amine system takes place with chemo-rheological changes that determine the kinetic behaviour of the system. Initially, the reaction kinetics is controlled by the chemical reactivity of the functional groups, but later on becomes controlled by diffusion and the degree of conversion levels off and tends to a limiting value. In these conditions, it is observed that the temperature of the glass transition equals the temperature of the curing reaction, $T_c$, and the properties of the system are those of the glassy state. This phenomenon is the vitrification of the system, which may be characterised by conventional differential scanning calorimetry (DSC) [1,2]. More recently, temperature modulated DSC (TMDSC) has been revealed as a calorimetric technique which gives a better understanding of the vitrification. In epoxy–amine systems TMDSC allows to determine the interval of vitrification and to study the kinetics during the diffusion control regime, and facilitates the building of the typical temperature–time-transformation (TTT) cure diagrams [3–12]. The molecular dynamics during the macromolecular growth has also been studied by the measurement of the complex heat capacity [13].

Other dynamic thermal analysis techniques have also been used to study the crosslinking reactions. One of them is torsional braid analysis (TBA) [14], which has been used to determine the gelation and vitrification times in order to build the TTT and the constant-heating-rate (CHT) cure diagrams [15,16]. In addition, some electric techniques, such as dielectric relaxation spectroscopy (DRS), have been extensively used to study the molecular dynamics of the system during the crosslinking reaction using a wide interval of frequencies. A general review of the application of DRS to thermoset cure may be found in the works of Senturia and Sheppard [17] and Johari [18]. In addition to these reviews, the conductive and dipolar response during the isothermal curing of epoxide–amine systems has also been described by other authors [19–33]. In some of these studies, the molecular dynamics has been related to thermodynamic aspects of the reactive system by analysing the variation of the relaxation time during the reaction progress [19,20,25–28]. One common objective of these studies is to determine the relation between the dielectric response and the chemo-rheological events, such as gelation and vitrification, which occur during the network growth.

* Corresponding author. Tel.: +34-937-398-123; fax: +34-937-398-101.
*E-mail address:* montserrat@mmt.upc.es (S. Montserrat).

0032-3861/03/$ - see front matter © 2002 Elsevier Science Ltd. All rights reserved.
PII: S0032-3861(02)00745-0

Recently, the relationship between the vitrification and the dielectric relaxation has been analysed in terms of the kinetics controlled by the diffusion of the functional groups [29,30], based on a modified Cole's equation [34], a WLF type equation [32] or empirical equations [22,28]. Other authors have studied this relationship in terms of the intermolecular cooperativity and dipole dynamics [35–37].

In the present work, the curing reaction of an epoxy resin based on diglycidyl ether of bisphenol A (DGEBA) cured with a dicycloalquildiamine is studied by calorimetric and dielectric techniques. The calorimetric techniques used are conventional DSC and TMDSC. Both techniques give the evolution of the conversion degree during the cure, and allow us to calculate the reaction rate and to determine the kinetics of the chemical reaction. Additionally, TMDSC allows the determination of the interval of the vitrification, and the analysis of the kinetics when the reaction is diffusion-controlled. Furthermore, the dielectric measurements obtained through the permittivity and the dielectric loss factor give a dipolar response, which has been correlated with the vitrification determined using the dynamic heat capacity measured by TMDSC.

## 2. Experimental

### 2.1. Materials and sample preparation

The epoxy system studied was an epoxy resin based on DGEBA (Araldite LY564 from CIBA Speciality Chemicals) and cured with a diamine based on 4,4′-diamino-3,3′-dimethyldicyclohexyl methane (3DCM) (HY 2954 from CIBA Speciality Chemicals). The epoxy equivalent of the resin was 170 g eq.$^{-1}$. The resin and the amine were mixed in a stoichiometric ratio (weight ratio 100:35) at room temperature, stirred for 10 min and then degassed in a vacuum chamber for 10–15 min. Finally, the samples were enclosed in aluminium pans or spread on ceramic cells for calorimetric or dielectric analysis, respectively.

### 2.2. Calorimetric measurements

The temperature modulated DSC measurements were performed with a METTLER TOLEDO 821e equipped with an intracooler, and STAR© software was used for alternating DSC (ADSC) evaluation. The temperature and heat flow calibrations were performed by standards of indium and zinc. The modulation conditions used in the quasi-isothermal curing reaction were amplitude of 0.5 K and a period of 1 min. The non-isothermal ADSC experiments were performed at an underlying heating rate of 1 K min$^{-1}$, and the same modulation conditions as in isothermal experiments. In order to calibrate the heat flow signal, correct the amplitude and eliminate the cell asymmetry, a blank with an empty pan on the reference side and an empty pan plus a lid on the sample side was performed before the sample measurement. The DSC measurements were performed at the usual heating rates of 10 K min$^{-1}$, except for multiscan experiments where the range was from 2.5 to 20 K min$^{-1}$. The sample weight was approximately 8–10 mg. The calorimetric scans were performed with a nitrogen gas flow of 50 mL min$^{-1}$.

ADSC is the temperature modulated DSC technique, commercialised by Mettler–Toledo, whose fundamental aspects have been shown and discussed in other papers [10,38–40]. In the following text, we will refer to ADSC as the TMDSC technique used in this work. In the case of a sinusoidal modulation of amplitude $A_T$ and angular frequency $\omega$ (radian s$^{-1}$), the temperature as a function of time is given by the equation

$$T = T_o + q_o t + A_T \sin(\omega t) \tag{1}$$

where $T_o$ is the initial temperature and $q_o$ is the underlying heating rate. Additionally, the periodic variation of the heating rate is given by the equation:

$$q = q_o + A_T \omega \cos(\omega t) \tag{2}$$

The modulation of the temperature gives a periodic heat flow signal, which is shifted by a phase angle with respect to the periodic heating rate. This shift is a consequence of the heat flow transfer within the sample-pan-holders system and also of the kinetic process in the sample. The Fourier analysis of the cycles of the heat flow and the heating rate gives the following quantities:

(i) The total or average heat flow $\langle \phi \rangle$, which gives an average heat capacity $\langle C_p \rangle = \langle \phi \rangle / q_o$. This property practically corresponds to the heat capacity obtained by conventional DSC.

(ii) According to the approach suggested by Schawe [41], a complex heat capacity may be defined as $C_p^* = C_p' - iC_p''$, where $C_p'$ and $C_p''$ are, respectively, the real and imaginary parts of the heat capacity. The modulus of the heat capacity is defined by the ratio of the heat flow amplitude, $A_\phi$, and the heating rate amplitude, $A_q (A_q = A_T \omega)$ :

$$|C_p^*| = \frac{A_\phi}{A_q} \tag{3}$$

(iii) The real and imaginary parts of the heat capacity are, respectively, defined by the following equations:

$$C_p' = |C_p^*| \cos \delta \tag{4}$$

$$C_p'' = |C_p^*| \sin \delta \tag{5}$$

where $\delta$ is the phase angle, which is very small in the case of a relaxation process associated with the glass transition, as in the case of the vitrification. Then the values of $|C_p^*|$ and $C_p'$ are practically indistinguishable, and the shape of $C_p''$ is very similar to that of the phase angle.

The study of the chemical kinetics and the progress of the reaction is based on the measurements of the total heat flow, $\langle\phi\rangle$, which allows us to calculate the degree of conversion, $\alpha$, and the reaction rate, $d\alpha/dt$, as in conventional DSC. The study of the vitrification phenomenon is based on the evolution of $|C_p^*|$, or alternatively on the phase angle, as was shown in a previous paper [10].

### 2.3. Dielectric measurements

A dynamic electric analyser DEA 2970 from TA Instruments was used to measure in real time both the dielectric permittivity ($\epsilon'$) and the dielectric loss factor ($\epsilon''$) of the epoxy samples isothermally cured at different frequencies. The complex dielectric constant, $\epsilon^*$, may be expressed by a general equation:

$$\epsilon^* = \epsilon' - i\epsilon'' \tag{6}$$

where $\epsilon'$ is the permittivity, which is proportional to the capacitance and depends on the orientation polarization as a result of both the change in the dipole moment due to the chemical reaction and the concentration of dipoles due to the volume contraction during the curing reaction. The loss factor $\epsilon''$ is a measure of the energy loss. For epoxy resins with a low ionic concentration, $\epsilon'$ is determined only by the dipolar orientation polarization and $\epsilon''$ is determined by both the ionic conduction and dipolar reorientation [18]:

$$\epsilon'(\omega, T_c, t_c) = \epsilon'_d(\omega, T_c, t_c) \tag{7}$$

and

$$\epsilon''(\omega, T_c, t_c) = \epsilon''_d(\omega, T_c, t_c) + \epsilon''_i(T_c, t_c) \tag{8}$$

where $\epsilon''_d$ is the dipolar contribution to $\epsilon''$, $\epsilon''_i$ represents the contribution of the dc conductivity to $\epsilon''$, $\omega$ is the angular frequency ($\omega = 2\pi f$) of the applied electrical field, $f$ is the measuring frequency, and $T_c$ and $t_c$ are the curing temperature and time, respectively. The conductivity is related to the loss factor by the relation $\sigma = \epsilon'' e_o \omega$, where $e_o$ is the permittivity (8.85 pF m$^{-1}$) of free space. The conductivity can be expressed by the contribution of two components:

$$\sigma(\omega, T_c, t_c) = \sigma_{dc}(T_c, t_c) + \sigma_{ac}(\omega, T_c, t_c) \tag{9}$$

where $\sigma_{dc}$ is the direct current component attributed to pure conductive process, and $\sigma_{ac}$ is the alternative current component related to the dipolar relaxation. The alternative expression of $\epsilon^*$ may be derived from Eqs. (6)–(9), at a curing temperature, $T_c$:

$$\epsilon^*(\omega, T_c, t_c) = \epsilon'_d(\omega, T_c, t_c) - i[\sigma_{dc}(T_c, t_c) + \sigma_{ac}(\omega, T_c, t_c)]/\omega e_o \tag{10}$$

Dielectric measurements were performed using a ceramic single surface cell of 20 mm × 25 mm based on a coplanar interdigitated-comb-like electrode design. The values of $\epsilon'$ and $\epsilon''$ are calculated from the resulting current and the phase angle shift induced. The interval of data sampling was 5 s per point. The mixture of epoxy–amine prepared as described above was spread on the electrode surface, covering the entire interdigitated area. The isothermal curing measurements were performed at temperatures from 60 to 140 °C, under a nitrogen atmosphere with a gas flow of 500 mL min$^{-1}$. The settling time before the isothermal measurement was between 3 and 5 min in the range of temperatures between 60 and 140 °C, respectively. The dielectric permittivity and the dielectric loss factor were measured at nine frequencies in the interval from 10 Hz to 100 kHz. The time taken to scan the different frequencies was 1.2 min.

## 3. Results and discussion

### 3.1. Thermodynamic data

The calorimetric analysis was performed using both conventional DSC and TMDSC. The former was used basically to characterise the thermochemistry of the curing reaction and ADSC was the technique used to analyse the relaxation process, which occurs during the vitrification of the system, and to complete the kinetics analysis. The heat of curing, $\Delta H$, was determined by non-isothermal DSC curves performed at different heating rates. An average value of 440 J g$^{-1}$ was obtained from non-isothermal curves at heating rates between 2.5 and 20 K min$^{-1}$. This value is considered as the total heat of curing, which will be used to calculate the degree of conversion by the ratio of the partial heat of curing and this value. The glass transition temperature, $T_g$, of the resin was determined on a second DSC scan, performed at 10 K min$^{-1}$ immediately after the first scan, giving a value of 143 °C measured on the midpoint of the transition.

This epoxy shows a particular behaviour because the value of $T_g$, obtained by postcure at 10 K min$^{-1}$ after the isothermal curing at temperatures between 60 and 160 °C, is not higher than 120 °C. In addition, no residual heat of curing is detected when the postcure is extended to 260 °C [42]. Nevertheless, a final scan of this sample raises the $T_g$ to about 143 °C, which is the maximum $T_g$ of the system measured at 10 K min$^{-1}$. This behaviour was also reported by Verchere et al. [43], and is a consequence of the chemical structure of the diamine. The situation of the methyl group in a neighbouring position to the amine group yields a steric hindrance that prevents the reactivity of these amine groups. The practically full reaction of the amine groups is achieved after heating at temperatures up to 260 °C, giving a resin with a higher $T_g$. However, lower values of $T_g$ due to the thermal degradation of the system may be obtained using a final temperature higher than 260–290 °C [44]. A more complete study of the evolution of the $T_g$ of the

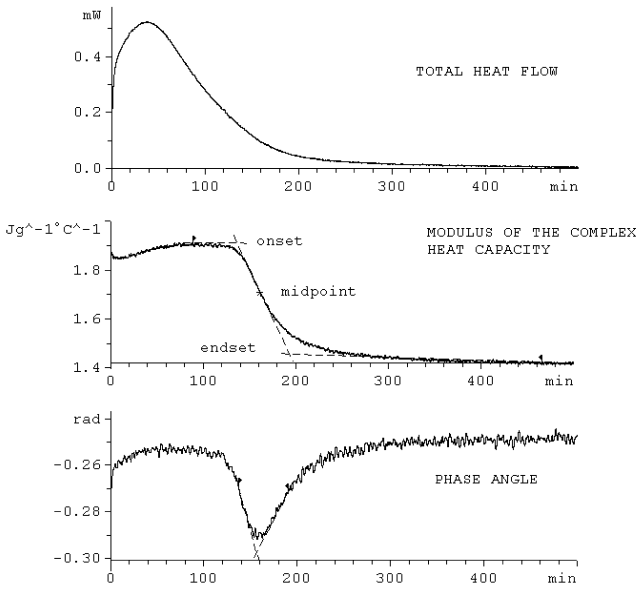


Fig. 1. ADSC curves (total heat flow, modulus of the complex heat capacity and phase angle) corresponding to the isothermal curing of the DGEBA-3DCM system at 60 °C. Modulation conditions: 0.5 K of amplitude and a period of 1 min. The time of vitrification at the extrapolated onset, midpoint and extrapolated endset are indicated in the curve of the modulus of the complex heat capacity. The curve of the phase angle shows the time corresponding to the extrapolated peak.

DGEBA-3DCM system during the isothermal and non-isothermal curing may be found in Refs. [42] and [44], respectively.

The temperature modulated DSC results have been analysed by the total heat flow, $\langle\phi\rangle$, the modulus of the complex heat capacity, $|C_p^*|$, and the phase angle, $\delta$, as shown in Fig. 1. As in conventional DSC, the total heat flow signal allows the calculation of the degree of conversion, $\alpha$, and furthermore the kinetic analysis of the chemical reaction. The isothermal curing was studied between 40 and 140 °C, but only the interval from 60 to 100 °C was used to study the evolution of the degree of conversion, which is shown in Fig. 2. At a temperature of 40 °C, the heat flow

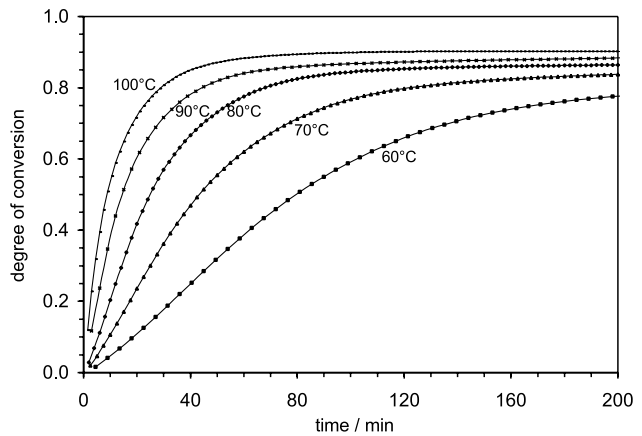


Fig. 2. Variation of the degree of conversion with the curing time for the indicated curing temperatures. The conversion degree values were obtained from the ADSC total heat flow data.

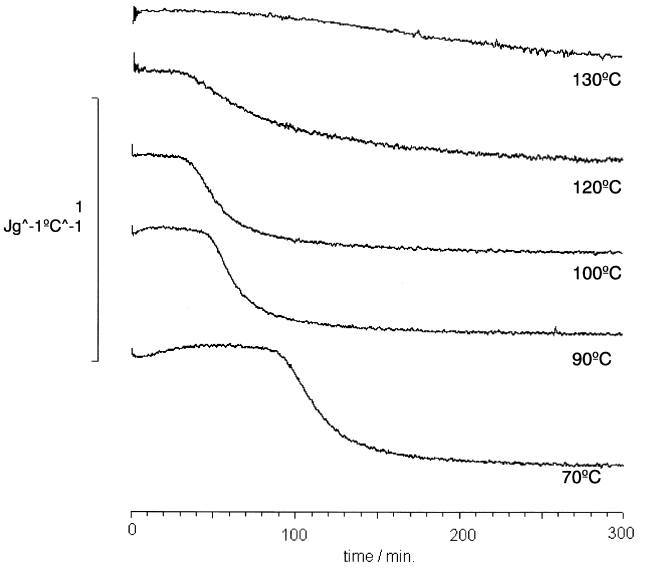


Fig. 3. Modulus of the complex heat capacity for the quasi-isothermal curing of the DGEBA-3DCM system at different temperatures (70, 90, 100, 120, and 130 °C). Modulation conditions: 0.5 K of amplitude and a period of 1 min.

signal is very small (maximum values about 0.1 mW were detected) and it is difficult to obtain reliable values of the degree of conversion. At temperatures higher than 100 °C, the exothermicity is concentrated at the beginning of the reaction. At this temperature, an uncontrolled amount of heat is lost during the interval of time elapsed between the introduction of the sample into the furnace of the calorimeter and the start of the recording of the heat flow values. We see in Fig. 2 that the degree of conversion of these isotherms, obtained at a curing temperature lower than the maximum $T_g$ of the resin is lower than unity as a consequence of the vitrification of the system.

The modulus of the complex heat capacity, $|C_p^*|$, shows a general trend characteristic of other epoxy–amine systems [3–5,8–10]. At the beginning, $|C_p^*|$ tends to increase slightly and in this case, levels off, presenting a plateau as shown for different curing temperatures in Fig. 3. According to Cassettari et al. [3], the initial increase in $|C_p^*|$ implies an increase of the number of configurational states or an increase of the vibrational modes during the growth of the linear chains. Further formation of the crosslinked structure as the reaction of the second amine group takes place may give a decrease in the number of configurational states, which induces a decrease in $|C_p^*|$, as was also observed in a diepoxide–polypropylenetriamine system [10]. In the present DGEBA-3DCM system, $|C_p^*|$ tends to be constant, probably due to the difficulties of the secondary amine groups in reacting [43].

After this smooth change, a drastic decrease in $|C_p^*|$ is observed which is attributed to the vitrification of the system [3–12]. As the crosslinked structure progresses and the system vitrifies, there is a characteristic time where the number of configurational states significantly decrease, and

Table 1
Vitrification properties (time and conversion degree) determined by ADSC from the complex heat capacity

| $T_c$ (°C) | $t_{v(o)}$ (min)[a] | $\alpha_{v(o)}$ | $t_v$ (min)[b] | $\alpha_v$ | $t_{v(e)}$ (min)[c] | $\alpha_{v(e)}$ | $\alpha_{limit}$ |
|---|---|---|---|---|---|---|---|
| 60 | 136.7 | 0.70 | 166 | 0.76 | 200 | 0.78 | 0.84 |
| 70 | 91.1 | 0.75 | 111.6 | 0.78 | 132 | 0.81 | 0.85 |
| 80 | 65.6 | 0.79 | 85.5 | 0.83 | 104.1 | 0.85 | 0.87 |
| 90 | 46.5 | 0.81 | 62.7 | 0.85 | 79.2 | 0.86 | 0.88 |
| 100 | 34.4 | 0.83 | 54.1 | 0.88 | 69.7 | 0.89 | 0.90 |
| 110 | 34 | – | 53.6 | – | 72.2 | – | – |
| 120 | 34 | – | 77.8 | – | 105 | – | – |
| 130 | 77 | – | ≈160 | – | ≈237 | – | – |

$T_c$ is the curing temperature.
[a] Time corresponding to the extrapolated onset of the vitrification.
[b] Time corresponding to the midpoint of the vitrification.
[c] Time corresponding to the extrapolated endset of the vitrification.

correspondingly there is an abrupt decrease in the heat capacity of the system. The reaction continues until the network structure becomes practically frozen in, and $|C_p^*|$ tends to acquire a constant value. The system undergoes a structural relaxation, going from a liquid state, corresponding to the highest value of $|C_p^*|$, to another state which is typical of a glass at the lowest value of $|C_p^*|$. This process corresponds to the vitrification of the system, where the kinetics is controlled by the diffusion of the reactive groups and, consequently, the degree of conversion seems to tend to a practically constant limiting value, as shown in Fig. 2 for different curing temperatures. The values of the limiting degree of conversion, $\alpha_{lim}$, are shown in Table 1.

These changes in the heat capacity allow one to determine the onset ($t_{v(o)}$) and endset ($t_{v(e)}$) of the vitrification, and consequently the interval of vitrification. At the same time, a vitrification time ($t_v$) may be empirically defined as the time at which the midpoint of

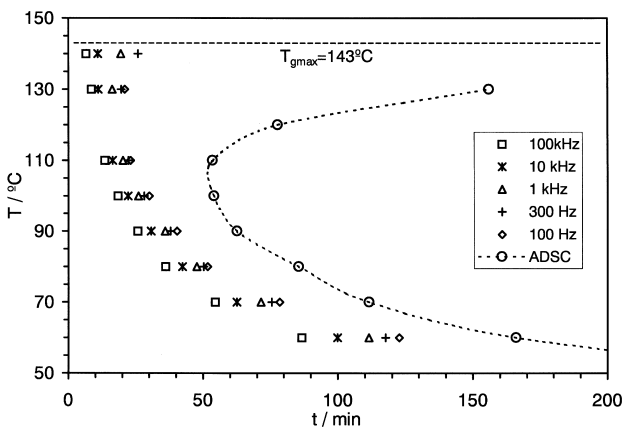


Fig. 4. Time–temperature-transformation cure diagram of DGEBA-3DCM system showing the vitrification times $t_v$ determined at different curing temperatures using the modulus of the complex heat capacity measured by ADSC (open circles). The dashed line is a guide for the eye. The plot also shows the times of the maximum of $\epsilon''$ at different frequencies, which are indicated in the inset. The maximum glass transition temperature of 143 °C was determined by DSC at 10 K min$^{-1}$ (see the text for details of the previous thermal history).

$\Delta|C_p^*|$ occurs, being

$$\Delta|C_p^*| = |C_p^*|(t_{v(o)}) - |C_p^*|(t_{v(e)}) \quad (11)$$

where $|C_p^*|(t_{v(o)})$ and $|C_p^*|(t_{v(e)})$ are the values of $|C_p^*|$ at the extrapolated onset and endset points. In a previous paper [10], it was shown that the values of the vitrification time are very similar to the values obtained by the method of partial curing, where $t_v$ is the time at which the midpoint $T_g$ of the resin equals $T_c$. Previous results of $t_v$ for this DGEBA-3DCM system from conventional DSC give a value of about 170 min (± 10 min), for a curing temperature of 60 °C [42]. This value lies in the interval of vitrification determined by ADSC (from 136.7 to 200 min), and agrees very well with the vitrification time of 166 min, determined at the midpoint of $\Delta|C_p^*|$. The vitrification times (including the onset and the endset values) and the corresponding degrees of conversion (determined from the total heat flow values) are shown in Table 1.

The values of the midpoint vitrification time allow the building of the vitrification line in the TTT cure diagram as shown by the open circles in Fig. 4. We see that for curing temperatures between 60 and 110 °C the vitrification time tends to decrease, but for higher temperatures it tends to increase. This shape is usual in other epoxy resins [14–16]. Nevertheless, because there is a significant difference between the highest $T_c$ at which the vitrification is clearly observable, which is about 130 °C, and the maximum glass transition of the resin, which is about 143 °C (measured at 10 K min$^{-1}$), the diagram seems to be incomplete. As mentioned above, this effect is a consequence of the steric hindrance of the amine groups, which prevents the fully isothermal cure of the resin, at this range of temperatures. At temperatures higher than 90 °C, the interval of vitrification becomes longer. From Fig. 3 and the values of Table 1, it is observed that the interval of vitrification is 33 min at 90 °C, and is about 160 min at 130 °C.

In addition, the $\Delta|C_p^*|$ in the vitrification, defined by Eq. (11), decreases when the temperature increases, as Fig. 5

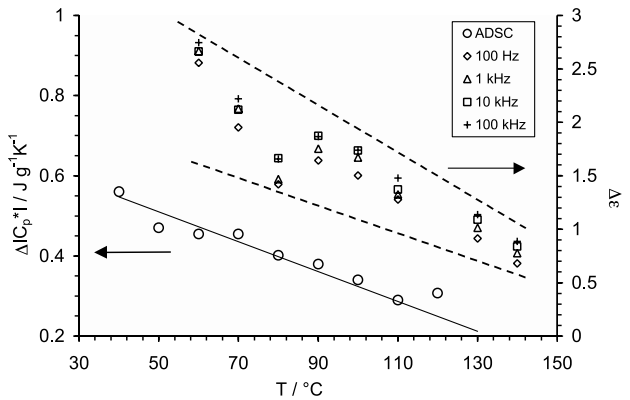


Fig. 5. Dependence of the variation of $|C_p^*|$ at vitrification on the curing temperature (open circles). The line corresponds to the linear regression fit of experimental data. The figure also shows the strength of the dipolar relaxation, $\Delta\epsilon = \epsilon_o - \epsilon_\infty$, obtained for different frequencies, which are indicated in the inset. The dashed lines are provided as a visual aid.

shows. This behaviour has also been reported in a diepoxide–polypropylenetriamine resin [10]. In the present DGEBA-3DCM resin, at a curing temperature of 130 °C, $\Delta|C_p^*|$ is very small, about 0.14 J g$^{-1}$ K$^{-1}$, and at higher temperatures it practically vanishes. In consequence, both effects, the long interval of vitrification and the small value of $\Delta|C_p^*|$, make the measurement of the vitrification time impossible at temperatures higher than 130 °C.

The phase angle between the heat flow and the heating rate, $\delta$, shows a peak in this region, which is the response to the relaxation process when the system changes to the glassy state (Fig. 1). The vitrification times may also be determined from the phase angle signal but a small advance in this times with respect to the times determined from $|C_p^*|$ may be detected [42].

### 3.2. Kinetic analysis of the curing reaction

As mentioned in Section 1, the curing kinetics is complex because during the crosslinking reaction the viscosity of the system increases and the kinetics, which is initially controlled by the chemical reactivity of the functional groups, becomes controlled by the diffusion of these groups in the medium. Finally, the conversion levels off and the system attains the glassy state. The beginning of the diffusion-controlled regime may be studied by kinetic analysis from the heat flow data. Furthermore, the measurement of the $|C_p^*|$ signal at a fixed frequency allows the determination of an interval of vitrification, as mentioned above. In this section, the comparison between the two properties is shown in order to check if the onset of vitrification matches the beginning of the diffusion-controlled regime. As will be shown in Section 3.3, this checking is fundamental in order to correlate the dielectric response and the calorimetric measurement by TMDSC.

The diffusion-controlled regime may be studied by a diffusion factor that depends on the degree of conversion and the temperature, DF($\alpha$,$T$), which is defined by the following ratio:

$$\mathrm{DF}(\alpha,T)=\frac{\left(\frac{\mathrm{d}\alpha}{\mathrm{d}t}\right)_{\mathrm{exp}}}{\left(\frac{\mathrm{d}\alpha}{\mathrm{d}t}\right)_{\mathrm{chem}}} \tag{12}$$

where $(\mathrm{d}\alpha/\mathrm{d}t)_{\mathrm{exp}}$ is the experimental reaction rate determined from the measurement of the total heat flow [$(\mathrm{d}\alpha/\mathrm{d}t)_{\mathrm{exp}}=\langle\phi\rangle/\Delta H$], and $(\mathrm{d}\alpha/\mathrm{d}t)_{\mathrm{chem}}$ is the reaction rate obtained from the fundamental equation of the kinetic analysis:

$$\frac{\mathrm{d}\alpha}{\mathrm{d}t}=k(T)f(\alpha) \tag{13}$$

In this equation, $k(T)$ is the rate constant, which is dependent on the temperature assuming an Arrhenius form, $k(T)=A\exp(-E_a/RT)$, where $A$ is the pre-exponential factor, $R$ is the gas constant and $E_a$ is the apparent activation energy, and $f(\alpha)$ is a function of the conversion degree. The apparent activation energy may be calculated by different methods from the heat flow curves as shown elsewhere [1,45].

The diffusion factor has been calculated in our DGEBA-3DCM system using two different functions of the degree of conversion, both of them corresponding to autocatalytic mechanisms. One function corresponds to the Sesták–Berggren model [46]:

$$f(\alpha)=\alpha^m(1-\alpha)^n \tag{14}$$

The kinetic parameters of this model may be calculated by the method proposed by Málek [47], which has been used in the kinetic analysis of other epoxy systems [10,45,48]. The apparent activation energy, $E_a$, was calculated previously by the isoconversional method [49] from the isothermal ADSC data. The values of $E_a$ change from 62.7 kJ mol$^{-1}$, for $\alpha=0.2$, to 51.7 kJ mol$^{-1}$, for $\alpha=0.7$. An average value of 57.9 kJ mol$^{-1}$ ($\pm$4.4 kJ mol$^{-1}$) is obtained, which agrees with the value reported by Verchere [43], namely between 56 and 59 kJ mol$^{-1}$. This value also agrees with that obtained by conventional DSC from the non-isothermal scans, which is 57.7 kJ mol$^{-1}$ ($\pm$0.6 kJ mol$^{-1}$), and by the Kissinger method of 58.7 kJ mol$^{-1}$. According to the method of Málek [47], $f(\alpha)$ is introduced into Eq. (13), and a value of the apparent activation energy of 58 kJ mol$^{-1}$ is substituted in the resulting equation. Then, a multilinear regression method allows us to determine the kinetic parameters ln $A$, $m$ and $n$. The analysis of the isotherm at 60 °C gives the following set of kinetic parameters: ln $A=12.99$, $m=0.47$ and $n=1.7$. These parameters allow the chemical reaction rate in the interval $0<\alpha<1$ to be calculated, and subsequently the diffusion factor at 60 °C, $\mathrm{DF}(\alpha,T)_{\mathrm{SB}}$, which is shown in Fig. 6. This diffusion factor shows a steady decrease from values of the extent of reaction between 0.65 and 0.70.

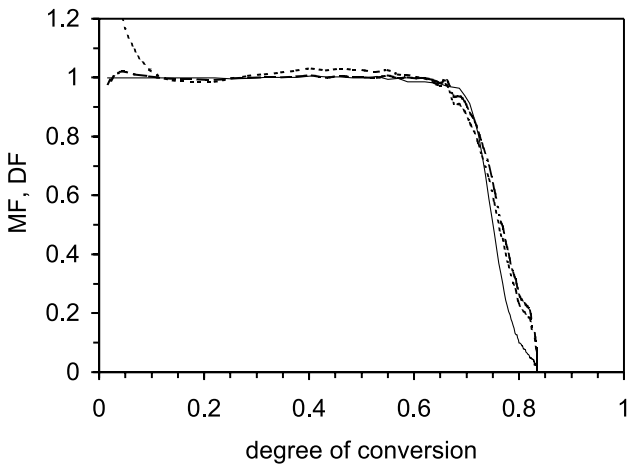


Fig. 6. Mobility factor MF($\alpha$,$T$) (—) and diffusion factor DF($\alpha$,$T$) calculated by the models of Sesták–Berggren (- - -) and Horie (–·–) for DGEBA-3DCM system at 60 °C. The MF($\alpha$,$T$) was obtained from the $|C_p^*|$ signal at the modulation conditions of 0.5 K of amplitude and a period of 1 min.

The diffusion factor was also calculated by the semiempirical equation proposed by Horie et al. [50]:

$$\frac{d\alpha}{dt} = (k_1 + k_2\alpha)(1-\alpha)^n \quad (15)$$

where $k_1$ and $k_2$ are temperature-dependent rate constants, and $n$ is an empirical reaction order. The fit of this equation to the experimental data of DGEBA-3DCM for $\alpha < 0.65$, at 60 °C, gives the following parameters: $k_1 = 7.09 \times 10^{-5}$ ($s^{-1}$), $k_2 = 5.03 \times 10^{-4}$ ($s^{-1}$) and $n = 2.04$. The diffusion factor calculated by this model $DF(\alpha,T)_H$ is also shown in Fig. 6. In the chemically controlled regime the $DF(\alpha,T)_H$ fits better than the $DF(\alpha,T)_{SB}$. In the vitrification region both factors show a similar trend.

The evolution of $|C_p^*|$ during vitrification may be expressed by a mobility factor $MF(\alpha,T)$, which is also conversion and temperature-dependent, introduced by Van Mele [5] to study the diffusion control regime and defined by the following equation:

$$MF(\alpha,T) = \frac{|C_p^*|(t,T) - |C_{p,g}^*|(T)}{|C_{p,l}^*|(t,T) - |C_{p,g}^*|(T)} \quad (16)$$

$MF(\alpha,T)$ is unity during the chemically controlled regime. It decreases in the vitrification interval, and vanishes when $|C_p^*|$ approaches the limiting value of the glassy state $|C_{p,g}^*|(T)$. For long curing times the value of $|C_p^*|$ tends to be constant, but sometimes, especially at low curing temperatures, a small variation is observed. In these cases, we take the lowest value of $|C_p^*|$ as $|C_{p,g}^*|(T)$. The evolution of $MF(\alpha,T)$ at 60 °C is shown in Fig. 6 for the DGEBA-3DCM system. It is observed that in the interval of vitrification the diffusion factor calculated by the models of Sesták–Berggren and Horie changes similarly to the mobility factor measured by ADSC. The fact that $DF(\alpha,T) \approx MF(\alpha,T)$ allows simulation of the experimental reaction rate by the product of the chemical reaction rate and the mobility factor:

$$\left(\frac{d\alpha}{dt}\right)_{sim} = \left(\frac{d\alpha}{dt}\right)_{chem} MF(\alpha,T) \approx \left(\frac{d\alpha}{dt}\right)_{chem} DF(\alpha,T) = \left(\frac{d\alpha}{dt}\right)_{exp} \quad (17)$$

The values of the simulated reaction rate for the Horie model, which are represented by open squares in Fig. 7, are in very good agreement with the experimental reaction rate (solid line in Fig. 7). This result indicates that in the DGEBA-3DCM system temperature modulated DSC provides a way to determine the beginning of the diffusion-controlled regime and to study the overall kinetic process. This conclusion was also reached in other epoxy–amine systems at the usual modulation conditions of 0.2–0.5 K of amplitude and a period of about 60 s [3–6,10,12].

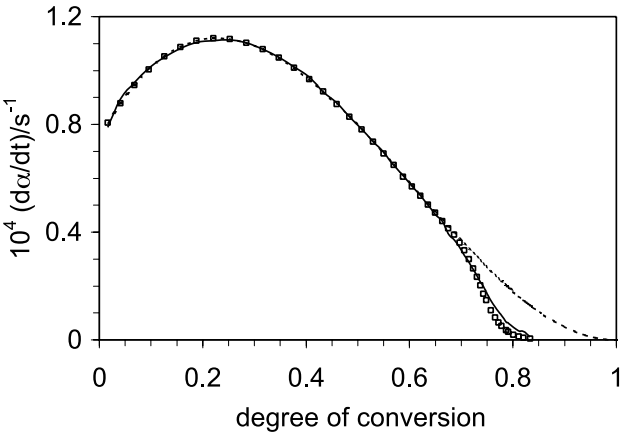


Fig. 7. Variation of the reaction rate against the degree of conversion, for the curing of the DGEBA-3DCM at 60 °C. The solid line (—) corresponds to the experimental values. The dashed line (- - -) represents the chemical kinetic values according to the Horie model, without mobility restrictions. The open squares corresponds to the simulated rate obtained by the product of the chemical kinetic values and the mobility factor.

### 3.3. Dielectric data

The dielectric experiments allow us to obtain the permittivity $\epsilon'(\omega,t_c)$ and the loss factor $\epsilon''(\omega,t_c)$ at different measuring frequencies and curing times $t_c$, for curing temperatures between 60 and 140 °C. Fig. 8a and b show

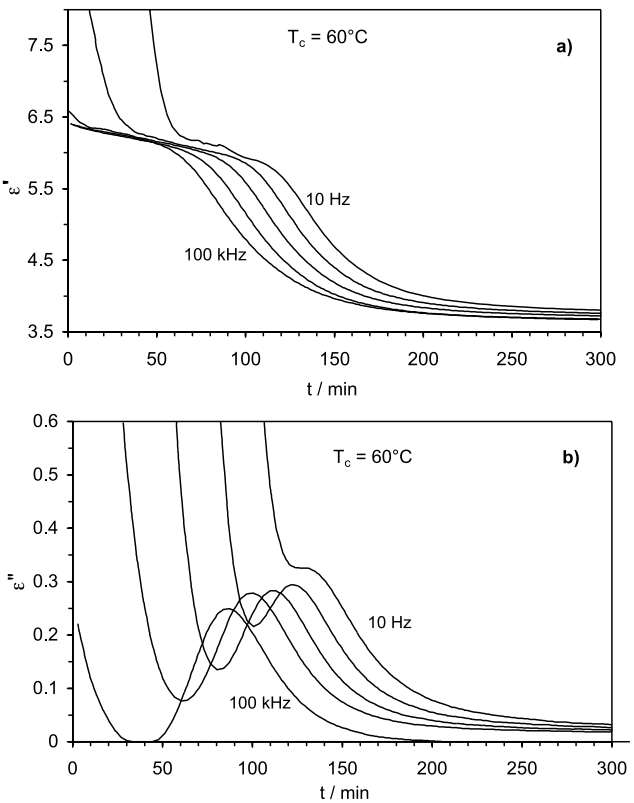


Fig. 8. Variation of the permittivity $\epsilon'$ (a) and loss factor $\epsilon''$ (b) with the curing time for the DGEBA-3DCM system at a curing temperature of 60 °C, and frequencies measured at each decade in the range 10 Hz to 100 kHz.

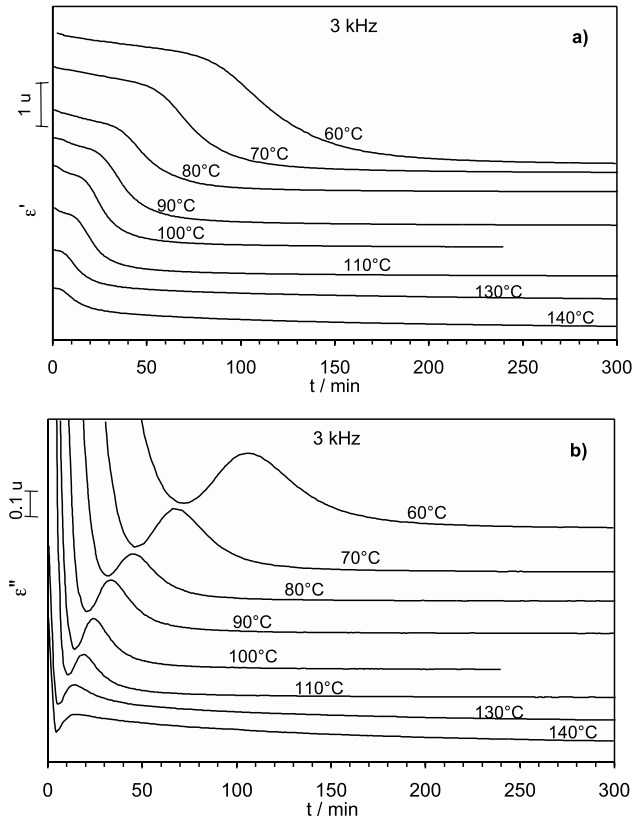


Fig. 9. Variation of the permittivity $\epsilon'$ (a) and loss factor $\epsilon''$ (b) with the curing time for the DGEBA-3DCM system at a frequency of 3 kHz and different curing temperatures between 60 and 140 °C. The $\epsilon'$ and $\epsilon''$ scales are relative, and curves are shifted vertically for clarity.

plots of $\epsilon'$ and $\epsilon''$, respectively, for frequencies between 10 Hz and 100 kHz at a curing temperature of 60 °C. It is observed that at the beginning of the reaction, the permittivity takes very large values and decreases drastically (Fig. 8a). This variation is attributable to an electrode polarization effect [17], due to the ionic impurities present in the reactants, epoxy resin and hardener, which are of commercial grade. This effect decreases as the measuring frequency increases and practically vanishes at a frequency of 1 kHz. At frequencies higher than 1 kHz, the curves of $\epsilon'$ are superposed, giving a value $\epsilon_o$, which is the relaxed permittivity of approximately 6.5, independent of the frequency. At the beginning of the reaction, $\epsilon'$ decreases slightly, almost reaching a plateau value, followed by a decay to a value of about 3.7. This is the so-called unrelaxed permittivity $\epsilon_\infty$, which tends to be practically constant for long curing times (Fig. 8a).

The loss factor $\epsilon''$ decreases with the curing time to reach a minimum, which is followed by a peak. The step decrease is attributed to the contribution of the dc conductivity to $\epsilon''$, which decreases as the reaction progresses. The subsequent increase is associated with the progressive increase in the ac conductivity as related to dipolar relaxation. The peak is observed as a consequence of the orientation polarization of the permanent electrical dipoles, which characteristic dipolar relaxation time, $\tau$, increases monotonically with curing time from a situation where $\omega\tau < 1$ to one in which $\omega\tau > 1$. The peak of dipolar relaxation is observed at the time in which $\omega\tau \approx 1$. The peak maximum in $\epsilon''$ appears at the same interval of time as the dispersion region in $\epsilon'$. Likewise, the maximum of $\epsilon''$ moves to higher curing times with decreasing frequency, as the peak is less defined at low frequency due to the superposition of dc conductivity, which is more significant at low frequencies, as is shown for 10 Hz at 60 °C in Fig. 8b. The general trends of $\epsilon'$ and $\epsilon''$ described for the curing of the DGEBA-3DCM system have also been observed in other curing reactions of epoxy resins [17–22,25,32].

The variation of the permittivity $\epsilon'$ with time shows a similar shape for other curing temperatures, as Fig. 9a shows for a frequency of 3 kHz. We see that the relaxation strength, $\Delta\epsilon = \epsilon_o - \epsilon_\infty$, of the dispersion region decreases and shifts to shorter curing times as the curing temperature increases. The values of $\Delta\epsilon$ for different frequencies and curing temperatures are shown in Fig. 5. It is observed that the variation of $\Delta\epsilon$ with temperature follows a tendency similar to the variation of $\Delta|C_p^*|$, also shown in Fig. 5.

In addition, the time of the maximum of the peak in $\epsilon''$, $t_m$, and the intensity (height) of the peak increase as the curing temperature decreases, as shown in Fig. 9b for the frequency of 3 kHz. However, $t_m$ tends to increase slightly when the temperature is 140 °C. This behaviour is more pronounced at low frequencies, as shown for 300 Hz at 140 °C in Fig. 4. The change of the variation of $t_m$ agrees with that observed in the vitrification time, $t_v$, obtained by ADSC, which is also shown in Fig. 4. Nevertheless, at low frequencies, the dipolar contribution in $\epsilon''$ is masked by the ionic or dc conductivity contribution. In order to study the dipolar relaxation associated with the peak in $\epsilon''$, a method proposed by Mangion and Johari [21] is applied to remove the ionic contribution. The method is based on the independence of the dc conductivity from the frequency and its decrease with the progress of the reaction, which may be described by a power law or an exponential function.

The dependence of the conductivity $\sigma(\omega, T, t_c)$ on the curing time for several frequencies between 10 and 1 kHz, at 60 °C, is shown in Fig. 10a. According to Eq. (9), the conductivity $\sigma(\omega,T,t_c)$ is the addition of the dc conductivity, $\sigma_{dc}(T, t_c)$, which is important at short curing times, and the ac conductivity, which is a consequence of the reorientation of dipoles in molecular segments, $\sigma_{dip}(\omega,T, t_c)$. The former $\sigma_{dc}$ is not dependent on the frequency and decreases with the increase in the curing time. The presence of a minimum in the conductivity curves at a time $t_{min}$ shows the dominant tendency of the dc conductivity for $t_c < t_{min}$, with $\sigma(\omega, T, t_c) \approx \sigma_{dc}(T, t_c)$, whereas the dipolar contribution is dominant for $t_c > t_{min}$ [21]. A very low dc contribution, strictly not null, is present at a slightly higher $t_c$ than $t_{min}$, but its effect is negligible. When the frequency decreases the minimum of these curves moves to longer times as a consequence of the larger significance of the dc conductivity at low frequencies. Alternatively, this minimum moves to shorter curing times when the curing temperatures increase.

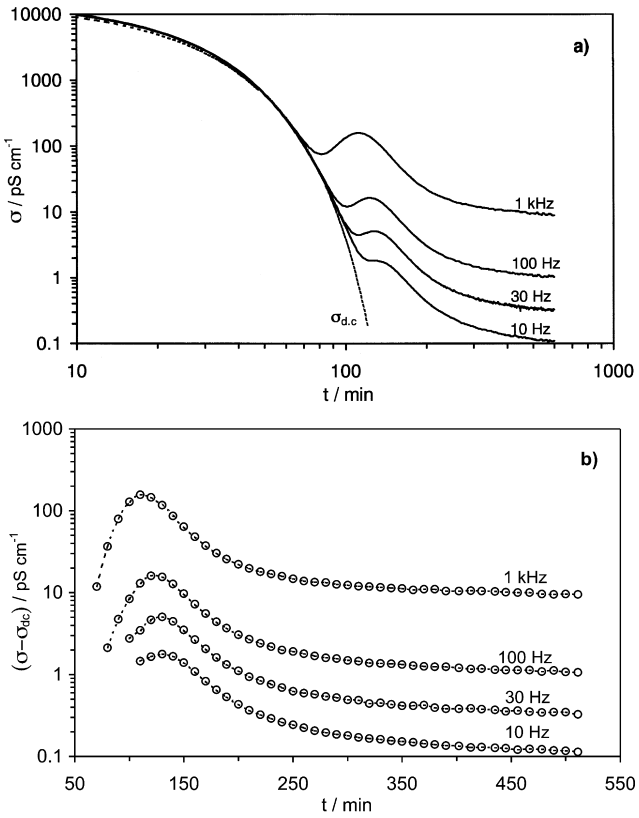


Fig. 10. (a) Variation of the conductivity $\sigma$ with the curing time for the DGEBA-3DCM system at 60 °C for different frequencies. The dashed line corresponds to the fit of the dc conductivity by Eq. (18). (b) Variation of $(\sigma - \sigma_{dc})$ with the curing time for the DGEBA-3DCM system at 60 °C for different frequencies. The dc conductivity has been calculated by the parameters of Table 2 for Eq. (18).

Relations between $\sigma_{dc}$ and the curing time have been reported by Mangion and Johari [21] and later applied to different curing reactions [22,23]. The relation applied in the present work is based on an exponential equation:

$$\sigma_{dc} = A \exp - \left[ \frac{B}{t_0 - t_c} \right] \quad (18)$$

where $A$, $B$ and $t_0$ are empirical constants whose values vary with temperature. At $t_c = t_0$ the dc conductivity reaches a singularity and $\sigma_{dc} = 0$. This time $t_0$ is formally longer than the vitrification time [22]. Values of $A$, $B$ and $t_0$ at different temperatures obtained by an iterative procedure using the $\sigma(\omega, t_c)$ data down to the minimum of the curve are listed in

Table 2
Fitting parameters of Eq. (18) to the dc conductivity measured during the isothermal curing of the DGEBA-3DCM system at different temperatures

| $T_c$ (°C) | $A$ (pS cm$^{-1}$) | $B$ (min) | $t_0$ (min) |
|---|---|---|---|
| 60 | $4.4 \times 10^{10}$ | 4135.5 | 278.35 |
| 70 | $1.4 \times 10^{10}$ | 1525.3 | 137.24 |
| 80 | $1.3 \times 10^{10}$ | 375.8 | 58.10 |
| 90 | $1.1 \times 10^{10}$ | 378.3 | 44.21 |
| 100 | $2.9 \times 10^{10}$ | 596.1 | 42.15 |

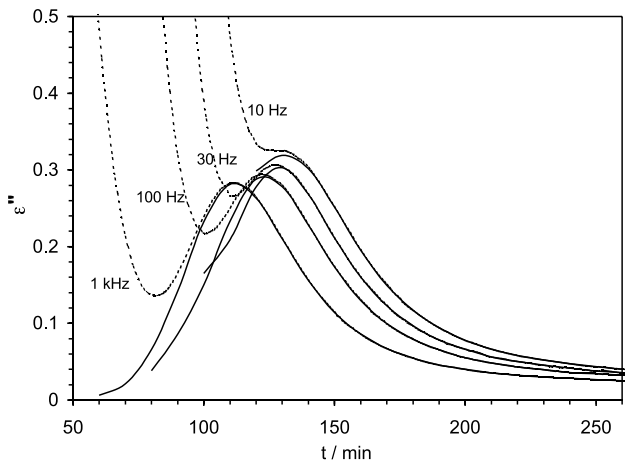


Fig. 11. Dependence of the dipolar loss factor (solid line) calculated from the conductivity corrected by the dc conductivity contribution, $(\sigma - \sigma_{dc})$, on the curing time for the DGEBA-3DCM system at 60 °C for different frequencies. The uncorrected curves of loos factor are also plotted (dashed lines).

Table 2. Fig. 10a shows the $\sigma_{dc}$ values calculated by Eq. (18) at 60 °C. The conductivity values corrected from the dc conductivity, $\sigma - \sigma_{dc}$, at 60 °C for different low frequencies are shown in Fig. 10b. These differences allow calculation of the dipolar loss factor, $\epsilon''_{dip}$, obtained from the equation $\epsilon''_{dip} = (\sigma - \sigma_{dc})/\omega e_0$ which are shown in Fig. 11 for different frequencies. The comparison between the corrected $\epsilon''_{dip}$ and the uncorrected $\epsilon''$ shows some differences in the position of the maximum peak, which is significant at low frequencies. The corrected times of the maximum in $\epsilon''$ have been used in the following discussion of the paper including the values shown in Fig. 4.

### 3.4. The dipolar relaxation associated with the vitrification of the system

In order to analyse the relation of the dipolar peak, observed by DRS, and the vitrification from the ADSC measurements we will focus the study on the evolution of two quantities: (i) the time of the maximum loss factor $\epsilon''$, $t_m$, which is frequency (and temperature) dependent, and (ii) the vitrification time, $t_v$, measured by ADSC at the midpoint of $|C_p^*|$. As mentioned above, the measurement of the $t_m$ was taken on the dipolar loss factor data, which was previously corrected from the ionic contribution.

First, we note a linear dependence of the logarithm of the frequency on $t_m$, for each curing temperature, as shown in Fig. 12. This dependence has also been observed before by other authors [19,29] and obeys the following equation:

$$f_m = f_m(0)\exp[-k_{dip} t_m] \quad (19)$$

and taking logarithms:

$$\log f_m = \log f_m(0) - \frac{k_{dip} t_m}{\ln 10} \quad (20)$$

where $f_m$ is the frequency of the maximum loss factor, and

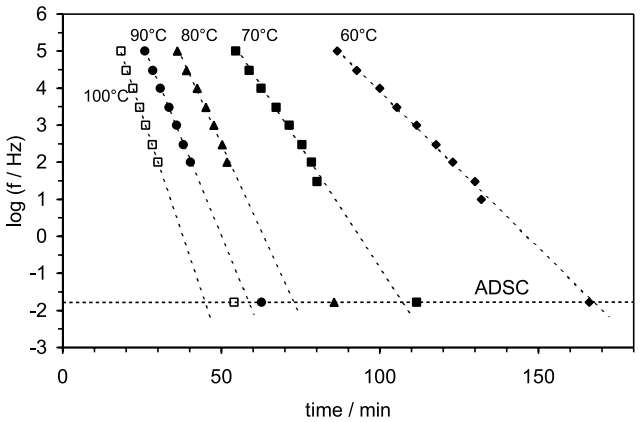


Fig. 12. Variation of the logarithm of the frequency with the time of the maximum loss factor at the indicated curing temperatures: 60 °C (◆), 70 °C (■), 80 °C (▲), 90 °C (•), and 100 °C (□). The dashed line corresponds to the fit of the dielectric data $\log f$ against $t_m$. The plot also includes the values of the vitrification time measured by ADSC from the modulus of the complex heat capacity $|C_p^*|$, which frequency of ADSC measurements is 16.7 mHz and $\log f_{ADSC} = -1.78$.

$f_m(0)$ and $k_{dip}$ are temperature-dependent constants, whose values are shown in Table 3. Whereas the frequency of the maximum loss may be related to an average relaxation time $[\langle\tau\rangle = 1/(2\pi f_m)]$, Eq. (19) indicates that $\langle\tau\rangle$ increases exponentially with time. The slope $k_{dip}$ tends to increase with the curing temperature, but near 130 °C there is a change and $k_{dip}$ decreases. This change has the same origin as that observed in the TTT diagram of Fig. 4 at 130 and 140 °C. At these temperatures, $t_m$ increases for lower frequencies.

In Fig. 12, together with the dielectric data of the maximum loss factor, the vitrification times measured by ADSC from the midpoint of the decay of $|C_p^*|$ are also plotted at temperatures between 60 and 100 °C. The frequency of ADSC measurements is 16.7 mHz, about three decades lower than the lowest frequency used in DRS (10 Hz). It is observed that at a curing temperature of 60, 70 and 90 °C, the ADSC data agree very well with the linear fit of $\log f_m$ against $t_m$, and at 80 and 100 °C there is a small deviation with respect to this fit. Notwithstanding this deviation, in the present epoxy system, the ADSC data at

Table 3
Dependence of the frequency on the time of maximum loss: temperature-dependent constants $f_m(0)$ and $k_{dip}$ according to Eq. (20)

| Curing temperature (°C) | $k_{dip}$ $10^3$ ($s^{-1}$) | $f_m(0)$ (Hz) | $r^2$ |
|---|---|---|---|
| 60 | 1.413 | $2.50 \times 10^{12}$ | 0.995 |
| 70 | 2.165 | $1.41 \times 10^{12}$ | 0.990 |
| 80 | 3.105 | $6.41 \times 10^{11}$ | 0.992 |
| 90 | 3.443 | $2.31 \times 10^{10}$ | 0.999 |
| 100 | 4.217 | $4.04 \times 10^{9}$ | 0.999 |
| 110 | 4.915 | $8.86 \times 10^{8}$ | 0.993 |
| 130 | 3.666 | $4.26 \times 10^{6}$ | 0.981 |
| 140 | 2.081 | $3.41 \times 10^{5}$ | 0.958 |

$r^2$ is the regression coefficient of the linear fit of Eq. (20).

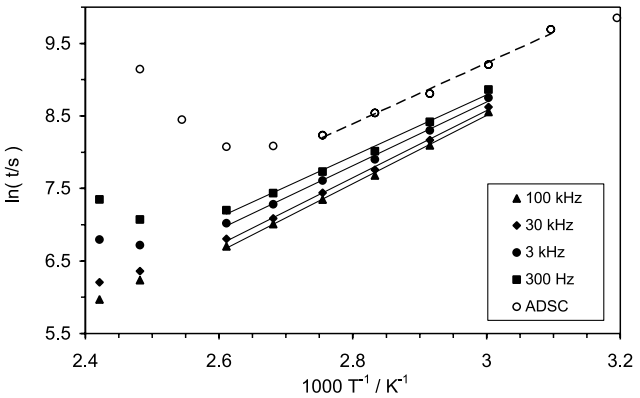


Fig. 13. Plot of the time of the maximum loss factor $t_m$ (filled symbols) and the vitrification time determined by ADSC $t_v$ (open circles) in logarithmic form against the reciprocal of the temperature, for different frequencies in the case of DRS and at 16.7 mHz for ADSC measurements. The solid lines correspond to the linear fits of the DRS data (between 60 and 110 °C) and the dashed line shows the linear fit of the ADSC data (between 50 and 90 °C).

16.7 mHz validate the linear extrapolation of $\log f_m$ measured by DRS at frequencies lower than 10 Hz.

In order to relate the dipolar relaxation to the kinetics of the crosslinking reaction, Mangion and Johari [19] have proposed an Arrhenius dependence of the curing time at the maximum peak loss factor for a given frequency, $t_m(f)$, expressed by the following equation:

$$t_m(f) = t_{m0}(f)\exp(E_{DRS}/RT) \quad (21)$$

where $t_{m0}$ $(f)$ is a pre-exponential factor and according to Ref. [19], $E_{DRS}$ represents an apparent activation energy of the chemical reaction. Both parameters $t_{m0}(f)$ and $E_{DRS}$ are frequency dependent. Fig. 13 shows the plot of $\ln[t_m(f)]$ against the reciprocal of curing temperatures between 60 and 140 °C for different frequencies in the range between 300 Hz and 100 kHz. A linear fit is observed and values of $E_{DRS}$ between 35 and 39 kJ $mol^{-1}$ were determined for these frequencies in the temperature range between 60 and 110 °C. Table 4 shows the values of $E_{DRS}$ at different frequencies. These values agree with those found by Williams and co-workers [29] in the DGEBA-PACM (4,4′-diaminodicyclohexylmethane) with an average value of 38.2 ± 2.9 kJ $mol^{-1}$ for measuring frequencies between 1 and 100 kHz. Mangion and Johari [19] found values of 47.1 and 44.5 kJ $mol^{-1}$ for DGEBA-DDM (4,4′-diaminodiphenyl methane) and DGEBA-DDS (4,4′-diaminodiphenil sulfone), respectively, for a frequency of 1 kHz.

However, at temperatures higher than 110 °C (or $T^{-1} < 2.61 \times 10^{-3}$ $K^{-1}$) and frequencies lower than 3 kHz a significant deviation with respect to the linear fit is obtained because $t_m$ tends to increase with the curing temperature, as was shown above in the TTT diagram in Fig. 4. Furthermore, a similar plot may be drawn using the vitrification times $t_v$ from $|C_p^*|$ measurements. The results are also shown in Fig. 13, and it is clear that $\ln t_v$ does not change linearly with the reciprocal of the curing temperature

Table 4
Apparent activation energy calculated from the relationship of $\ln[t_m(f)]$ with the reciprocal of the curing temperature by the use of ADSC and DRS data

| Frequency (kHz) | Technique | Interval of temperatures | Apparent activation energy (kJ mol$^{-1}$) |
|---|---|---|---|
| $16.7 \times 10^{-6}$ | ADSC | 50–90 | 35.0 |
| 0.1 | DRS | 60–110 | 34.9 |
| 0.3 | ,, | ,, | 35.1 |
| 1 | ,, | ,, | 35.9 |
| 3 | ,, | ,, | 36.5 |
| 10 | ,, | ,, | 38.4 |
| 30 | ,, | ,, | 38.4 |
| 100 | ,, | ,, | 39 |

in the range between 40 and 140 °C. The vitrification times measured by ADSC tend to decrease with the $T_c$, but about 100 °C this tendency changes and $t_v$ increases with $T_c$. This change is a consequence of the opposing effects of the increase in the reaction rate and the decreasing concentration of reactants at vitrification as $T_c$ approaches the maximum glass transition of the system [14]. Nevertheless, assuming an Arrhenius type equation for the ADSC vitrification times, $t_v$, in the interval of temperatures between 50 and 90 °C, similar to Eq. (21) [$t_v = t_{v0} \times \exp(E_{ADSC}/RT)$], an apparent activation energy $E_{ADSC}$ of 35 kJ mol$^{-1}$ may be calculated. We note that this value is very similar to that of $E_{DRS}$ obtained by $t_m$ values, at temperatures between 60 and 110 °C.

Notwithstanding this problem with the limitation of the range of temperature, we can proceed to determine whether these apparent activation energies, $E_{DRS}$ or $E_{ADSC}$, correspond to an apparent activation energy of the chemical reaction, $E_a$. As mentioned above, the value of $E_a$ found by the isoconversional method applied to the isothermal ADSC data in the chemical reaction regime decreases with the increase in the degree of conversion, and an average value of $E_a = 57.9$ kJ mol$^{-1}$ is obtained [42]. The value of $E_{ADSC}$, which is determined in the diffusion-controlled regime, is significantly lower than that determined during the chemical reaction. A similar behaviour has also been observed by other authors [51,52] during the curing of an epoxy resin. On the other hand, the isoconversional method compares the time to reach the same degree of conversion at different temperatures, while the determination of $E_{ADSC}$ is performed by comparing chemical states of different degrees of conversion. The $E_{DRS}$ values are similar to that obtained by ADSC. Predictably, it seems that they do not correspond to an apparent activation energy of the chemical reaction.

In order to obtain a better understanding of the correlation between the dipolar relaxation and the thermal relaxation induced by the vitrification of the system, in this section the dielectric data will be related to the progress and the kinetics of the reaction. Prior to the present work, there have been many attempts to relate the dipolar dielectric response of the system to the chemical and physical changes that occur during the crosslinking of the system [22,27–30,36,37]. In particular, the work of Williams and co-workers [29] quantitatively shows that the curing of the system DGEBA–PACM becomes diffusion-controlled at times corresponding to the maximum value of the loss factor at measuring frequencies $f \leq 1$ Hz. These authors use a diffusion factor, calculated by a modified Cole's equation [34], which corrects the chemical reaction rate calculated by an empirical function of the conversion. Other authors [22,28] propose the use of an empirical equation for the variation of the relaxation time against the degree of conversion.

In this paper, the $|C_p^*|$ signal obtained by ADSC is used in an attempt to establish a quantitative relation between dielectric relaxation and the beginning of the diffusion-controlled reaction. The discussion is based on the following points:

(i) As the reaction progresses, the time scale of the molecular motions increases due to the crosslinking of the system. Consequently, the measuring frequency to detect the dipolar relaxation associated with the molecular dynamics of the system decreases as the degree of conversion increases. At a determined time scale, which may be of the order of 100 s [53], the system vitrifies and the conversion levels off. In these conditions the kinetics comes under control by diffusion.
(ii) The onset of the vitrification of the DGEBA-3DCM system may be detected at the point where the experimental reaction rate deviates from the chemical reaction rate, or in other words when the diffusion factor becomes lower than 1. This deviation is a consequence of the diffusion-controlled regime. As shown above, the diffusion factor is identified with the mobility factor defined by the relative change of $|C_p^*|$ given by Eq. (16). This identity allows the detection of the beginning of the diffusion-controlled regime by the onset of the decrease in MF($\alpha$, $T$).
(iii) According to the results shown in Fig. 12, it is assumed that the plot of logarithm of the frequency against $t_m$ is linear within the range of $f_m$ comprised between 100 kHz and 16.7 mHz.

At a fixed curing temperature, the frequency of the maximum loss $f_m$ (where the dielectric absorption reaches its maximum) may be expressed as a function of the degree

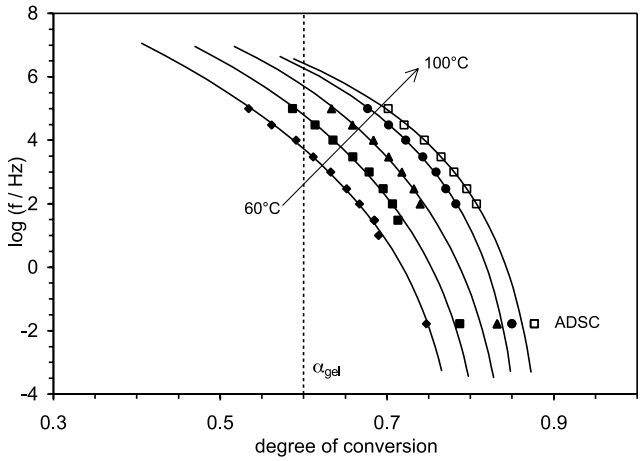


Fig. 14. Plot of the logarithm of the frequency against the degree of conversion at the maximum loss factor for the following curing temperatures: 60 °C (◆), 70 °C (■), 80 °C (▲), 90 °C (•), 100 °C (□). As in Fig. 12, the symbols at $\log f = -1.78$ correspond to the measurements by ADSC. The solid line corresponds to the continuous variation of the logarithm of the frequency calculated by the Eq. (20) and further relation with the degree of conversion as indicated in the text. The vertical line at a conversion of 0.6 corresponds to the $\alpha_{gel}$ [43].

of conversion. Instead of using a phenomenological function of $f(\alpha)$ to relate $\alpha$ and $t$, we use the measured values of $\alpha$–$t$, calculated previously by the total heat flow of ADSC curves (shown in Fig. 2). The time to reach a determined degree of conversion was obtained from the $\alpha$–$t$ data and then substituted in Eq. (20) to obtain the corresponding value of $\log f_m$. The variation of the logarithm of the frequency against the degree of conversion at the maximum loss factor for different $T_c$ is shown by solid lines in Fig. 14. In the same figure, the experimental points corresponding to the maximum loss factor, and at a lower frequency, the value obtained from $|C_p^*|$ measured by ADSC are also plotted.

The shape of the curves of $\log(f_m)$ versus $\alpha$ in the range between 100 kHz and 16.7 mHz agrees with that observed by Williams et al. in the same interval of $f_m$ ([29; figs. 12 and 14]). The extrapolation of these curves to frequencies above 100 kHz was not performed in the present work because there are no experimental data available to validate this range. Nevertheless, Fig. 14 shows a short extrapolation to $10^7$ Hz, which gives a quasi-linear variation of $\log(f_m)$ versus $\alpha$, more clearly observed at 60 and 70 °C, that agrees with the results of Williams et al. [29].

The $\log(f_m)$ decreases steadily with the degree of conversion. In the range of the dielectric frequencies, the variation of $\log(f_m)$ with $\alpha$ is slower than in the range between 10 Hz and 16.7 mHz. The frequency changes from 2.5 decades per 1/10 of $\alpha$ in the former range, to a change of about five decades per 1/10 of $\alpha$, in the latter range. According to Verchere et al. [43], the conversion at the gel point for this DGEBA-3DCM is about 0.6, therefore at 60 and 70 °C the gelation takes place in the range of the dielectric measuring frequencies. At values of the degree of conversion corresponding to this range, the dielectric relaxation includes the growth of the chain, the gelation process and further crosslinking of the network. In this frequency range, at 60 °C, the conversion degree varies from 63 to 82% of the $\alpha_{(lim)}$, and at 100 °C from 78 to 90% of the $\alpha_{(lim)}$. The final values of the degree of conversion of this range are very close to those of the onset of vitrification measured by ADSC, which are 83 and 92% of $\alpha_{(lim)}$ at 60 and 100 °C, respectively, according to the values shown in Table 1.

In the range where the change of $\log(f_m)$ with the degree of conversion is steeper, approximately between the lower frequencies of DRS (about 10–100 Hz) and the frequency of ADSC measurements (16.7 mHz), the system enters the glassy state. The degree of conversion corresponding to the vitrification times (midpoint values) measured by ADSC are 90 and 97% of $\alpha_{(lim)}$ at 60 and 100 °C, respectively. The calorimetric data indicate that the beginning of the diffusion-controlled regime takes place in this range. According to points (ii) and (iii) above, the comparison between the mobility factor and the curves of $\log(f_m)$ versus $\alpha$ allows the correlation of the dipolar relaxation with the diffusion-controlled regime. This comparison is shown in Fig. 15a and b for $T_c = 60$ and 100 °C, respectively. In these figures, the degree of conversion corresponding to the decay of MF($\alpha$, $T$) determines the degree of conversion at the onset of vitrification, $t_{v(o)}$, and consequently the beginning of the diffusion-controlled kinetics. At the temperatures of 60 and 100 °C the frequency which corresponds to $\alpha$ at $t_{v(o)}$ is 9 and 7 Hz, respectively. For other temperatures between 60 and 100 °C, this frequency is ≤15 Hz. Therefore, we can establish that in the DGEBA-3DCM system, the time at which the reaction becomes diffusion-controlled corresponds to the time of the maximum $\epsilon''$ obtained at a frequency lower than or equal to 15 Hz, in the range of curing temperatures between 60 and 100 °C. This result differs only one decade with respect to the value determined by Williams et al [29] in the DGEBA-PACM system ($f \leq 1$ Hz). This difference may be attributed to the different reactivity of the epoxy–diamine system, which involves different molecular dynamics, and also to the particular methodology used to determine the beginning of the diffusion-controlled step.

The dipolar peaks shown at the highest frequencies correspond to the relaxation of the system for a determined degree of conversion or crosslinking, which may be relatively far from the value of the onset of vitrification determined by ADSC. For instance, this is the case of a measuring frequency of 100 kHz, where at 60 °C the maximum of the loss peak appears at 88 min with a degree of conversion of $\alpha = 0.54$. At this degree of conversion the kinetics is chemically controlled since the onset of vitrification is detected by ADSC for $\alpha = 0.70$.

## 4. Conclusions

In this paper, we have presented the isothermal curing of

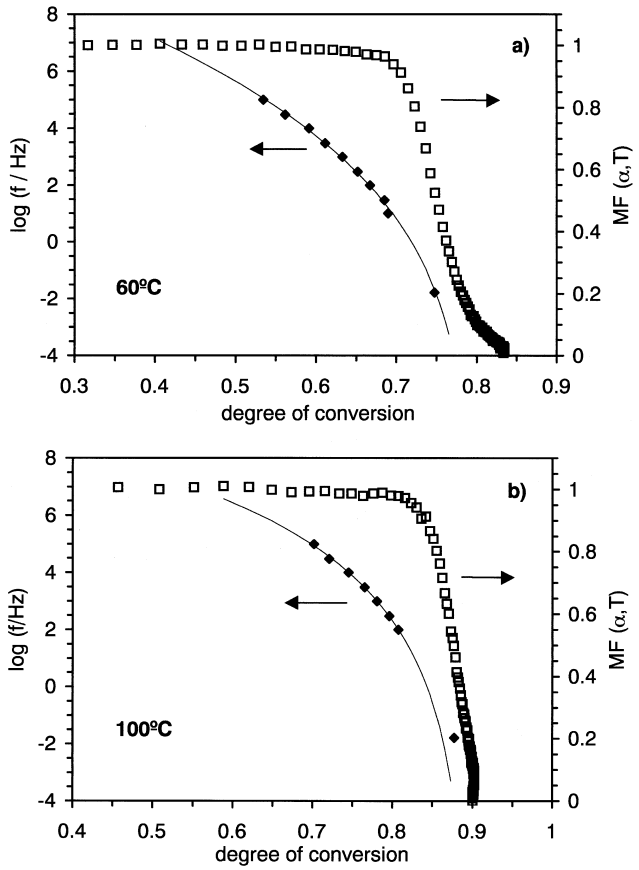


Fig. 15. Plots of logarithm of the frequency (◆) and mobility factor (□) against the degree of conversion at the maximum loss factor for the curing temperature of 60 °C (a) and 100 °C (b). ADSC modulation conditions: 0.5 K of amplitude and a period of 1 min. The solid line corresponds to the continuous variation of the logarithm of the frequency calculated by Eq. (20) and further relation with the degree of conversion as indicated in the text.

an epoxy resin based on DGEBA with a diamine based on 4,4′-diamino-3,3′-dimethyldicyclohexylmethane (3DCM) analysed by DRS, conventional DSC and TMDSC. The calorimetric data obtained by DSC allowed us to determine an average heat of curing of 440 J $g^{-1}$, and to analyse the glass transition temperature of the resin. In accordance with other authors [43], the difficulty of measuring the $T_g$ of the 'fully' cured epoxy is attributable to the steric hindrance of the amine groups, which prevents us from obtaining the fully cured epoxy by isothermal reaction. The total heat flow obtained by ADSC was used to determine the degree of conversion and the vitrification was determined by the decay of the $|C_p^*|$. The chemical kinetics corresponds to an autocatalytic model with an average apparent activation energy of 58 kJ $mol^{-1}$. The model of Horie fits better than the model of Sesták–Berggren in the chemically controlled regime. In the vitrification region, where the kinetics is diffusion-controlled, the diffusion factor DF($\alpha$,$T$) defined by the ratio of the experimental reaction rate and the chemical reaction rate may be identified with the mobility factor MF($\alpha$,$T$), which is defined by the relative change of $|C_p^*|$ (Eq. (16)). This identity, which was proven in the DGEBA-3DCM system for the modulation conditions of the ADSC experiments ($A_T = 0.5$ K, period = 60 s), allows the detection of the beginning of the diffusion-controlled regime by the decay of MF($\alpha$, $T$).

The dielectric results of the permittivity and the loss factor show behaviour similar to that of other epoxy–amine systems, but some particular differences are observed as a consequence of the hindered reactivity of the diamine. The dipolar relaxation, analysed by the peak of the maximum loss factor, was correlated with the thermal relaxation associated with vitrification, which is analysed by the variation of the $|C_p^*|$ signal. The ADSC data confirm the validity of the extrapolation of the loss factor peak to lower frequencies in the plot of log ($f_m$) against $t_m$. The calorimetric $\alpha$–$t$ data allow to study the variation of the log($f_m$) versus the degree of conversion at the maximum loss factor. The curves of log($f_m$) − $\alpha$ in the range of the experimental frequencies (100 kHz to 16.7 mHz) show two different tendencies with characteristic molecular dynamics. In the range of the dielectric frequencies the degree of conversion corresponds to the growth of the chain, the gelation for $T_c$ of 60 and 70 °C, and further crosslinking of the network close to the vitrification of the system. In the range of frequencies between the lower dielectric $f_m$ and the ADSC, the slope is steeper and the system vitrifies.

Assuming that the beginning of the diffusion-controlled regime is determined by the onset in the decay of the mobility factor, it is observed that the dipolar peaks measured at the lowest frequencies (10–30 Hz) are very close to the onset of vitrification. The comparison of the dielectric and ADSC data allows us to establish that in the DGEBA-3DCM system, the time of the maximum $\epsilon''$ of the dipolar peaks obtained at measuring frequencies lower than (or equal to) 15 Hz corresponds to the time at which the kinetics becomes controlled by diffusion. These results show that the mobility factor obtained by ADSC is a quantitative indicator to correlate the dielectric response with the thermal relaxation associated with the vitrification of this epoxy–amine system.

## Acknowledgements

Financial support has been provided by CICYT (MAT97-0634-C02-02) and DGI (MAT2000-1002-C02-01). The authors are grateful to CIBA Speciality Chemicals for supplying the epoxy and the hardener. One of us (F.R.) acknowledges a grant from the MEC (SB99-002221691) to collaborate in this project.

## References

[1] Prime B. In: Turi EA, editor. Thermal characterization of polymeric materials, vol. 2. San Diego: Academic Press; 1997. Chapter 6.
[2] Williams RJJ. In: Stepto RFT, editor. Polymer networks, principles of

their formation, structure and properties. London: Chapman & Hall; 1998. Chapter 4.
[3] Cassettari M, Salvetti G, Tombari E, Veronesi S, Johari GP. J Polym Sci: Polym Phys 1993;31:199.
[4] Van Assche G, Van Hemelrijck A, Rahier H, Van Mele B. Thermochim Acta 1995;268:121.
[5] Van Assche G, Van Hemelrijck A, Rahier H, Van Mele B. Thermochim Acta 1997;304/305:317.
[6] Van Assche G, Verdonck E, Van Mele B. Polymer 2001;42:2959.
[7] Tatsumiya S, Yokokawa K, Miki K. J Therm Anal 1997;49:123.
[8] Swier S, Van Assche G, Van Hemelrijck A, Rahier H, Verdonck E, Van Mele B. J Therm Anal 1998;54:585.
[9] Tombari E, Ferrari C, Salvetti G, Johari GP. Chem Phys 1998;230: 267.
[10] Montserrat S, Cima I. Thermochim Acta 1999;330:189.
[11] Jenninger W, Schawe JEK, Alig I. Polymer 2000;41:1577.
[12] Schawe JEK. Thermochim Acta 2000;361:97.
[13] Ferrari C, Salvetti G, Tombari E, Johari GP. Phys Rev E 1996;54: R1058.
[14] Enns JB, Gillham JK. J Appl Polym Sci 1983;28:2567.
[15] Aronhime MT, Gillham JK. Adv Polym Sci 1986;78:84.
[16] Wisanrakkit G, Enns JB, Gillham JK. J Appl Polym Sci 1990;41: 1895.
[17] Senturia SD, Sheppard NF. Adv Polym Sci 1986;80:3.
[18] Johari GP. In: Ellis B, editor. Chemistry and technology of epoxy resins. Glasgow: Chapman & Hall; 1996. Chapter 6.
[19] Mangion MBM, Johari GP. J Polym Sci: Polym Phys 1990;28:1621.
[20] Mangion MBM, Johari GP. Macromolecules 1990;23:3687.
[21] Mangion MBM, Johari GP. J Polym Sci: Polym Phys 1991;29:1117.
[22] Wasylyshyn DA, Johari GP. J Polym Sci: Polym Phys 1997;35:437.
[23] Butta E, Livi A, Levita G, Rolla PA. J Polym Sci: Polym Phys 1995; 33:2253.
[24] Sheppard NF, Senturia SD. Polym Engng Sci 1986;26:354.
[25] Koike T. J Appl Polym Sci 1992;44:679.
[26] Deng Y, Martin GC. J Polym Sci: Polym Phys 1994;32:2115.
[27] Cassettari M, Salvetti G, Tombari E, Veronesi S, Johari GP. J Noncrystall Solids 1994;172–174:554.
[28] Tombari E, Ferrari C, Salvetti G, Johari GP. Phys Chem: Chem Phys 1999;1:1965.
[29] Fournier J, Williams G, Duch C, Aldridge GA. Macromolecules 1996; 29:7097.
[30] Williams G, Smith IK, Holmes PA, Varma S. J Phys: Condens Matter 1999;11:A57.
[31] Williams G, Smith IK, Aldridge GA, Holmes PA, Varma S. Polymer 2001;42:3533.
[32] Bartolomeo P, Chailan JF, Vernet JL. Polymer 2001;42:4385.
[33] Alig I, Jenninger W, Junker M, de Graaf LA. J Macromol Sci: Phys 1996;B35:563.
[34] Cole KC, Hecher S-J, Noël D. Macromolecules 1991;24:3098.
[35] Andjelic S, Fitz B, Mijovic J. Macromolecules 1997;30:5239.
[36] Fitz B, Mijovic J. Macromolecules 1999;32:4134.
[37] Fitz B, Mijovic J. Macromolecules 2000;33:887.
[38] Hutchinson JM. Thermochim Acta 1998;324:165.
[39] Jiang Z, Imrie CT, Hutchinson JM. Thermochim Acta 1998;315:1.
[40] Montserrat SJ. Therm Anal Cal 2000;59:289.
[41] Schawe JEK. Thermochim Acta 1995;261:183.
[42] Montserrat S, Martín G. J Appl Polym Sci 2002;85:1263.
[43] Verchère D, Sautereau H, Pascault JP, Riccardi CC, Moschiar SM, Williams RJJ. Macromolecules 1990;23:725.
[44] Montserrat S, Martín GJ. Thermochim Acta 2002;388:343.
[45] Montserrat S, Andreu G, Cortés P, Calventus Y, Colomer P, Hutchinson JM, Málek J. J Appl Polym Sci 1996;61:1663.
[46] Sesták J, Berggren G. Thermochim Acta 1971;3:1.
[47] Málek J. Thermochim Acta 1992;200:257.
[48] Montserrat S, Málek J. Thermochim Acta 1993;228:47.
[49] Friedman HL. J Polym Sci: Part C 1964;6:183.
[50] Horie K, Hiura H, Sawada M, Mita I, Kambe H. J Polym Sci Part A-1 1970;8:1357.
[51] Stutz H, Mertes J, Neubecker K. J Polym Sci: Polym Chem 1993;31: 1879.
[52] Vyazovkin S, Sbirrazzuoli N. Macromolecules 1996;29:1867.
[53] Kovacs AJ, Aklonis JJ, Hutchinson JM, Ramos AR. J Polym Sci: Polym Phys 1979;17:1097.